Using Impedance to Track Fracture Healing Rates in Mice *In Vivo*: A Pilot Study*

Monica C. Lin, Diane Hu, Frank Yang, Safa T. Herfat, Chelsea S. Bahney, Meir Marmor, and Michel M. Maharbiz, *Member, IEEE*

***Abstract*— Fracture injuries are highly prevalent worldwide, with treatment of problematic fractures causing a significant burden on the U.S. healthcare system. Physicians typically monitor fracture healing by conducting physical examinations and taking radiographic images. However, nonunions currently take over 6 months to be diagnosed because these techniques are not sensitive enough to adequately assess fracture union. In this study, we display the utility of impedance spectroscopy to track different healing rates in a pilot study of an *in vivo* mouse tibia fracture model. We have developed small (56 µm) sensors and implanted them in an externally-stabilized fracture for twice-weekly measurement. We found that impedance magnitude increases steadily over time in healing mice but stalls in non-healing mice, and phase angle displays frequency-dependent behavior that also reflects the extent of healing at the fracture site. Our results demonstrate that impedance can track differences in healing rates early on, highlighting the potential of this technique as a method for early detection of fracture nonunion.**

I. Introduction

Fracture injuries are highly prevalent worldwide, with impaired healing occurring in up to 20% of patients [1]. Furthermore, treatment of these problematic fractures cost an estimated $45 billion to the U.S. healthcare system in 2008 [2]. While physician examination and radiographic imaging are the most common methods for assessing fracture union, these techniques are not sensitive enough, particularly in the early stages of healing when lack of tissue mineralization limits the utility of X-rays [3]–[5]. There is a need for an objective measurement tool to monitor fracture healing and distinguish between the early stages of healing, as this can inform rehabilitation decisions and determine the need for intervention in cases of fracture nonunion.

Electrical impedance spectroscopy provides a simple and low-cost method to quantitatively characterize multiple tissue types [6]–[8], and multiple studies have shown promising data within the context of fracture healing [9]–[13]. In addition, we have previously shown in a cadaver model that impedance spectroscopy measurements can distinguish between different types of tissues present in healing fractures, such as blood, cartilage, trabecular bone, and cortical bone [14]. In an *ex vivo* mouse study examining calluses dissected from unstable fractures, we found that impedance magnitude and phase angle at multiple frequencies have significant correlations with volume fractions of cartilage and trabecular bone within a callus [15]. However, limitations of these studies include noise arising from electrode insertion required after a sample has already been dissected out of the specimen. This underscores the need for sensors to be implanted *in vivo*, so fractures can heal around the electrodes and concerns about poor contact between electrodes and tissues can be abated.

In this study, we present our design of sensors for use in a mouse tibia fracture model, as well as our results from a pilot study examining how impedance spectroscopy measurements can be used to characterize fracture states over the course of healing.

II. Methods

A. System Overview

We developed a measurement system consisting of a custom user interface that communicates with control hardware to step through a specified list of frequencies and records impedance magnitude (|Z|) and phase angle (θ) [16]. 2-point impedance measurements were taken from 20 Hz to 1 MHz with a 100 mV constant voltage sine wave output signal using a Keysight Technologies E4980AL Precision LCR Meter.

To create a sensor small enough to implant in a mouse leg, where the tibia measures approximately 1 mm in diameter, we used 25.4 µm-diameter Platinum wire insulated with 1.27 µm of isonel (for a total diameter of 27.94 µm). 2 wires were cut to approximately 50 mm in length, and a small 175 µm section of insulation in the center of the wires was burned off using a CO_2 laser. These 2 wires were then offset so the 2 exposed sections serving as electrodes were spaced 0.5 mm apart, and then twisted together to form a single sensor. In addition, the wires were coiled on either side of the electrodes to allow for strain relief, as shown in Fig. 1A.

B. Mouse Model

Approval was obtained from the UCSF Institutional Animal Care and Use Committee (IACUC) prior to performing this mouse study. Fractures were made in the mid-diaphyses of mice tibias and stabilized using custom-

*Research supported by the National Science Foundation (NSF) under grant no. EFRI-1240380, an NSF Industry/University Cooperative Research Program called the Center for Disruptive Musculoskeletal Innovations under grant IIP-1361975, and the Orthopaedic Trauma Association.

M. C. Lin is with the Bioengineering Department at the University of California – Berkeley, CA 94720 and the University of California – San Francisco, CA 94158 USA (phone: 408-799-0730; email: monica.lin@berkeley.edu).

D. Hu, F. Yang, S. T. Herfat, C. S. Bahney, and M. Marmor are with the Department of Orthopaedic Surgery at the University of California – San Francisco / Zuckerberg San Francisco General Hospital Orthopaedic Trauma Institute, San Francisco, CA 94110 USA (emails: Diane.Hu@ucsf.edu, Frank.Yang@ucsf.edu, Safa.Herfat@ucsf.edu, Chelsea.Bahney@ucsf.edu, Meir.Marmor@ucsf.edu).

M. M. Maharbiz is with the Electrical Engineering & Computer Science and the Bioengineering Departments at the University of California – Berkeley, CA 94720 USA (email: maharbiz@eecs.berkeley.edu).

designed external fixators (Fig. 1B) in 6 wild-type C57BL/6 mice. The sensors were then carefully placed in the fracture gap, with skin sutured around the ends of the sensors, leaving wire ends available for connection to measurement instrumentation, as seen in Fig. 1C. 1 mouse was found dead on day 4 and taken out of the study. To monitor the progression of healing, mice were anesthetized twice weekly for measurements on days 0, 4, 7, 11, 14, 18, 21, 25, and 28. In between measurements, a thin but rigid acrylic sheath was placed over the external fixator to protect the sensor from damage. At each time point, 3 sets of measurements were taken of each fracture, with each set involving 5 impedance measurements taken at 18 frequencies chosen over a range of 20 Hz to 1 MHz. X-ray images were also taken using a Hologic Fluoroscan Premier Encore 60000 C-Arm Imaging System at every time point (Fig. 1D).

C. Histology

Samples were fixed after measurement in 4% paraformaldehyde (pH 7.2) overnight (4°C), then decalcified in Cal-Ex for 2 days. Tissue was then dehydrated through a graded ethanol series and embedded in paraffin. Serial 10 µm longitudinal sections were collected throughout each sample and stained with Hall's and Brunt's Quadruple (HBQ) stain, which stains cartilage tissue blue and bone red.

D. Data Analysis

Both impedance magnitude and phase have been normalized to account for variation between sensors and samples, and enable comparison of healing between multiple mice. The day 0 measurement was removed due to the instability of the fracture on the day of surgery along with the flexibility of the small sensor enabling some motion immediately following surgery. Instead, the data was normalized as a ratio to the next earliest time point (day 4), to ensure that the sensor and fracture had time to stabilize so there was no additional motion between the sensor and the fractured bone ends for the remainder of the study.

III. Results and Discussion

A. Histology and fluoroscopy indicates 2 healing patterns

In this model, the majority of new bone forms through endochondral ossification, which progresses through 4 stages of healing. A hematoma is first produced (Stage 1), followed by a cartilage intermediate (Stage 2).This callus becomes mineralized and is converted into trabeculated bone (Stage 3), before finally being remodeled into cortical bone (Stage 4). In mice, we expect complete healing by day 28.

We completed histology for all 5 mice in the study, and found that their resultant state of healing at day 28 diverged into 2 groups. 2 of the mice developed a robust callus, with clear signs of healing as seen in Fig. 2A. However, the other 3 mice displayed poor signs of healing, with their fracture gaps dominated by fibrous tissue, as seen in Fig. 2B. We believe that this difference in healing is likely due to movement of the sensor. While the sensor was designed to be flexible and very small in size relative to the mouse tibia and fracture callus to minimize obstruction of healing, this flexibility also resulted in probable movement of the sensor relative to the fractured bone ends and surrounding soft tissue. This increased movement at the fracture site likely led to the overabundance of fibrous tissue, resulting in an atrophic nonunion with complete absence of bony bridging found in 3 of the mice. In 2 of the mice, any movement was likely minimal, allowing for development of a robust callus with clear bony bridging. This was supported by X-ray images taken immediately after surgery as well as at the time of euthanasia. The X-rays for the 2 healing mice showed that on day 28, the sensor appeared unchanged and in the same location as on day 0. However X-rays for the 3 non-healing mice showed that on day 28, the coils flanking the exposed electrodes were no longer present, a clear indication that the sensor moved from its original position. However, an advantage of these small sensors is that they are able to be preserved throughout the histology process and can be sectioned along with the tissue. Fig. 2C shows an image of the sensor's precise placement within the tissue, and illustrates the clear integration of the sensor within the fracture tissues.

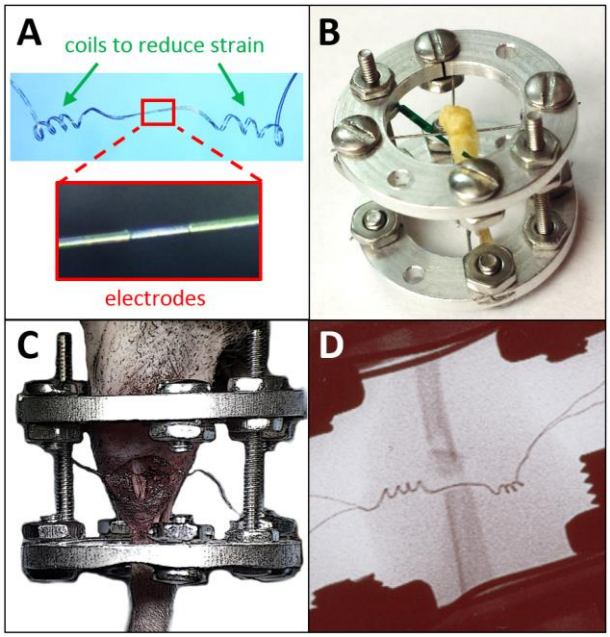

Figure 1. A) 58 µm sensor made from thin Pt wire, with 2 insulated regions serving as electrodes. **B)** External fixator used to stabilize a mouse tibia fracture in our model. **C)** Sensor implanted at the fracture site in a mouse tibia. **D)** X-ray of sensor implanted in the fracture gap.

B. Impedance tracks differences between healing and non-healing mice

Normalized |Z| and θ have been plotted over time for each of the samples at 1 kHz and 100 kHz, shown in Fig. 3A and 3B, respectively. At both of these frequencies, |Z| increases with fracture progression as expected in the healing cases, and stalls in the non-healing cases. At lower frequencies such as 1 kHz, the healing fractures display a normalized θ consistently less than 1, indicating that θ is becoming less negative over healing time. Conversely, the non-healing cases display a normalized θ greater than 1, indicating that θ is becoming more negative over healing time. The opposite trends are found at higher frequencies such as 100 kHz. These results align well with our previous studies in which |Z| increases from blood to cartilage to bone, and θ becomes less negative as cartilage converts to bone at low frequencies and more negative as cartilage converts to bone at high frequencies, shown both in

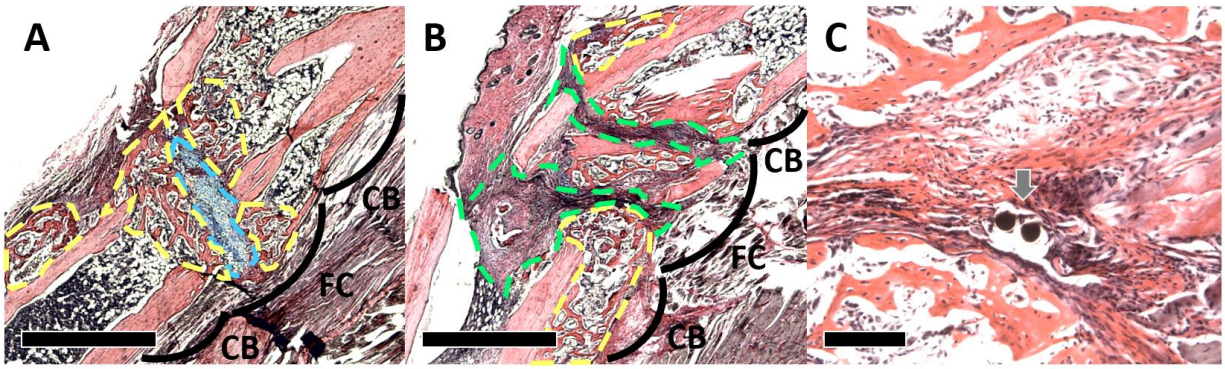

Figure 2. A-B) Histology of a healing mouse (A) and a non-healing mouse (B), stained with HBQ. CB = Cortical Bone, FC = Fracture Callus. Dashed outlines: Blue = cartilage, Yellow = new bone, Green = fibrous tissue. Scale bar = 1 mm. **C)** Gray arrow points to sensor embedded in fracture tissue. Scale bar = 0.1 mm.

cadaveric studies [14] and *ex vivo* mouse studies [15]. This is because tissues in the early stages of healing (blood, cartilage) are more conductive than those in the late stages (trabecular and cortical bone), leading to rising |Z| over healing time. In addition, bone is comprised of matrix layers that can be modeled as capacitors, leading to the resultant trends in θ. Importantly, we start to see differences between the 2 groups of mice almost immediately, with |Z| for the healing mice rising at a faster rate than for the non-healing mice. Similarly, θ seems to deviate very quickly from the original normalized value of 1 as well. This indicates the ability of impedance measurements to quickly identify stalled healing as compared to a traditional technique such as X-ray, which is only able to detect mineralized tissue at late healing stages.

To understand differences in frequency response for the 2 healing patterns, we plotted normalized |Z| and θ as a function of frequency early on in healing (day 7), as seen in Fig. 4A, and late in healing (day 28), as seen in Fig. 4B. The non-healing samples have relatively flat frequency responses relative to their initial behavior on day 4, while the healing cases show a clear jump in |Z|, particularly from 1 kHz to 100 kHz relative to day 4. Again, this is in line with previous studies showing that the greatest spread in |Z| across days occurs in this frequency range. This reveals that formation of a robust callus influences the frequency response of the measurement, providing additional quantitative evidence from which to characterize the state of the fracture.

Finally, to understand how impedance tracks healing progression over time, we look in detail at how the frequency response shifts as a result of healing or lack thereof. Fig. 5A shows a series of plots that track frequency response for a healing mouse over the course of the study, with Fig. 5B showing an analogous graph for a non-healing mouse. In the healing mice, we observe clear shifts in the frequency response as the fracture moves through the healing stages over time, especially between 5 kHz and 100 kHz. However, in the mice suffering from nonunion, we see that the frequency response remains largely unchanged over time, with minimal differences compared to the healing mice. This underscores the potential of impedance to quickly discern when a fracture is not healing properly and is instead getting stuck in the early stages of healing.

IV. Conclusion

Currently, fracture nonunion often takes over 6 months to diagnose because physicians rely on subjective examination and radiography to monitor healing, where the non-mineralized early stages are particularly difficult to track. In

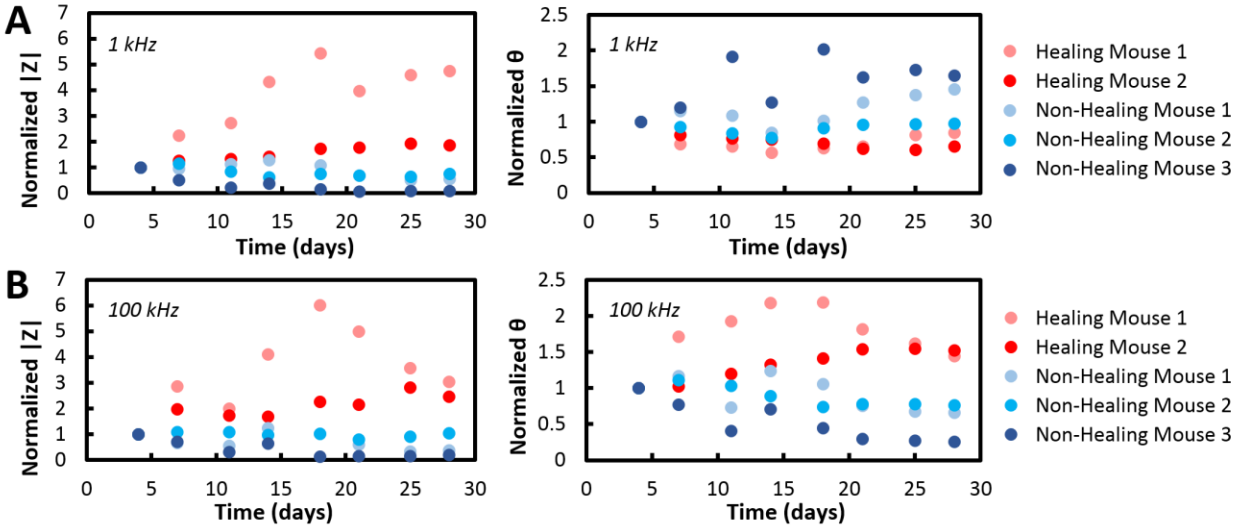

Figure 3. A-B) Normalized |Z| and θ plotted over the course of fracture healing at 1 kHz (A) and 100 kHz (B).

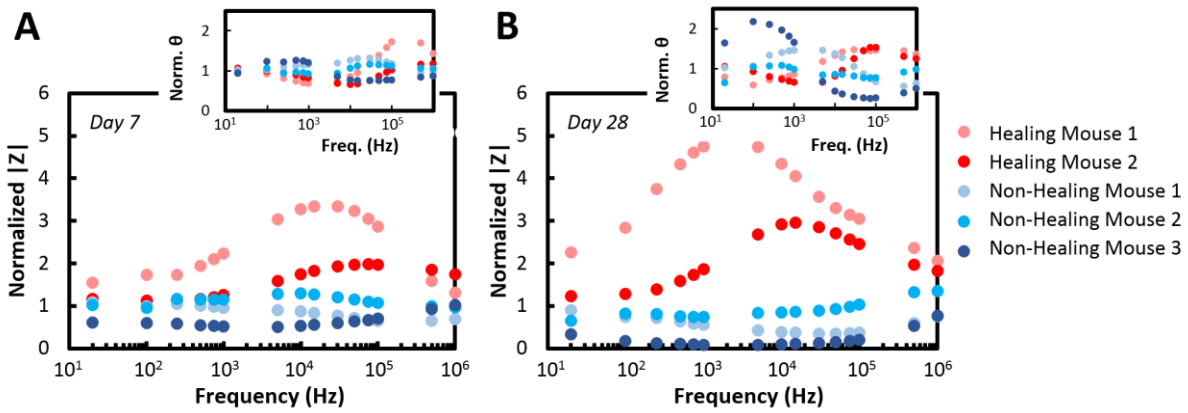

Figure 4. A-B) Normalized |Z| and θ (inset) plotted over a range of frequencies from 20 Hz to 1 MHz at day 7 (A) and day 28 (B) post-fracture.

this study, we sought to quantify the progression of fracture healing especially in the early stages, and were able to delineate between impedance measurements taken across healing fractures that have developed a robust callus and non-healing fractures that lack signs of bony bridging. Not only can we see clear differences in |Z| and θ over time at a given frequency between these 2 groups, but we can track how the frequency responses of these measurements change over time depending on the type of healing confirmed through histology.

While these results support the use of impedance to track fracture healing, this study is limited by the fact that presence of a sensor within the fracture gap likely contributed to a greater fibrotic response than in a typical externally-fixed fracture without a sensor. Since this issue is primarily a result of sensor movement relative to the fracture bone ends, work is currently underway to explore alternate forms of fixation such as using a bone plate that would limit the impact of a sensor to the healing process and thus curb excess fibrotic response. Ultimately, this sensor could potentially be incorporated as a small instrumented screw that is added to the current internal fixation procedure.

ACKNOWLEDGMENT

We acknowledge support from the Berkeley Sensor and Actuator Center, the Swarm Lab at UC Berkeley, the Orthopaedic Trauma Institute at Zuckerberg San Francisco General Hospital. M. C. L. was supported by a National Science Foundation Graduate Research Fellowship.

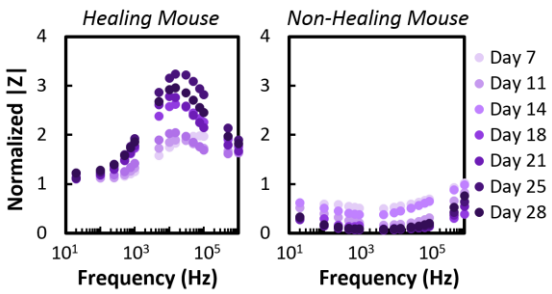

Figure 5. Frequency responses of normalized |Z| over the course of fracture healing for a healing mouse and a non-healing mouse.

REFERENCES

[1] C. Lu, E. Meinberg, R. Marcucio, and T. Miclau, "Fracture repair and bone grafting," *OKU 10 Orthop. Knowl. Update*, pp. 11–21, 2011.

[2] American Academy of Orthopaedic Surgeons, "The Burden of Musculoskeletal Diseases in the United States," Bone and Joint Decade, 2008.

[3] S. Morshed, "Current Options for Determining Fracture Union," *Adv. Med.*, vol. 2014, pp. 1–12, 2014.

[4] S. P. Whiley, "Evaluating fracture healing using digital x-ray image analysis," *Contin. Med. Educ.*, vol. 29, no. 3, p. 102, 2011.

[5] V. C. Protopappas, M. G. Vavva, D. I. Fotiadis, and K. N. Malizos, "Ultrasonic monitoring of bone fracture healing," *IEEE Trans. Ultrason. Ferroelectr. Freq. Control*, vol. 55, no. 6, pp. 1243–1255, Jun. 2008.

[6] R. D. Stoy, K. R. Foster, and H. P. Schwan, "Dielectric properties of mammalian tissues from 0.1 to 100 MHz; a summary of recent data," *Phys. Med. Biol.*, vol. 27, no. 4, p. 501, 1982.

[7] D. A. Dean, T. Ramanathan, D. Machado, and R. Sundararajan, "Electrical impedance spectroscopy study of biological tissues," *J. Electrost.*, vol. 66, no. 3–4, pp. 165–177, Mar. 2008.

[8] S. Gabriel, R. Lau, and C. Gabriel, "The dielectric properties of biological tissues: II. Measurements in the frequency range 10 Hz to 20 GHz," *Phys Med Biol*, vol. 41, pp. 2251–2269, 1996.

[9] T. Yoshida, W.-C. Kim, Y. Oka, N. Yamada, and T. Kubo, "Assessment of distraction callus in rabbits by monitoring of the electrical impedance of bone," *Acta Orthop.*, vol. 81, no. 5, pp. 628–633, Oct. 2010.

[10] S. Kumaravel and S. Sundaram, "Monitoring of fracture healing by electrical conduction: A new diagnostic procedure," *Indian J. Orthop.*, vol. 46, no. 4, p. 384, 2012.

[11] K. Gupta, P. Gupta, G. K. Singh, S. Kumar, R. K. Singh, and R. N. Srivastava, "Changes in electrical properties of bones as a diagnostic tool for measurement of fracture healing," *Hard Tissue*, vol. 2, no. 1, p. 3, 2013.

[12] I. Ritchie and V. Kulkarni, "Impedance osteography: clinical applications of a new method of imaging fractures," *J. Biomed. Eng.*, vol. 12, pp. 369–374, Sep. 1990.

[13] E. Kozhevnikov, X. Hou, S. Qiao, Y. Zhao, C. Li, and W. Tian, "Electrical impedance spectroscopy – a potential method for the study and monitoring of a bone critical-size defect healing process treated with bone tissue engineering and regenerative medicine approaches," *J Mater Chem B*, vol. 4, no. 16, pp. 2757–2767, 2016.

[14] M. C. Lin, S. T. Herfat, C. S. Bahney, M. Marmor, and M. M. Maharbiz, "Impedance spectroscopy to monitor fracture healing," presented at the IEEE EMBC, 2015, pp. 5138–5141.

[15] M. C. Lin, F. Yang, S. T. Herfat, C. S. Bahney, M. Marmor, and M. M. Maharbiz, "New Opportunities for Fracture Healing Detection: Impedance Spectroscopy Measurements Correlate to Tissue Composition in Fractures," *J. Orthop. Res.*, Apr. 2017.

[16] S. L. Swisher *et al.*, "Impedance sensing device enables early detection of pressure ulcers in vivo," *Nat. Commun.*, vol. 6, p. 6575, Mar. 2015.